# Distinct modes of derepression of an *Arabidopsis* immune receptor complex by two different bacterial effectors

Yan Ma[a,1,2], Hailong Guo[a,1], Lanxi Hu[a,3], Paula Pons Martinez[a], Panagiotis N. Moschou[a,4], Volkan Cevik[a,5], Pingtao Ding[a], Zane Duxbury[a,6], Panagiotis F. Sarris[a,7], and Jonathan D. G. Jones[a,8]

[a]The Sainsbury Laboratory, NR4 7UH Norwich, United Kingdom

Plant intracellular nucleotide-binding leucine-rich repeat (NLR) immune receptors often function in pairs to detect pathogen effectors and activate defense. The *Arabidopsis* RRS1-R–RPS4 NLR pair recognizes the bacterial effectors AvrRps4 and PopP2 via an integrated WRKY transcription factor domain in RRS1-R that mimics the effector's authentic targets. How the complex activates defense upon effector recognition is unknown. Deletion of the WRKY domain results in an RRS1 allele that triggers constitutive RPS4-dependent defense activation, suggesting that in the absence of effector, the WRKY domain contributes to maintaining the complex in an inactive state. We show the WRKY domain interacts with the adjacent domain 4, and that the inactive state of RRS1 is maintained by WRKY–domain 4 interactions before ligand detection. AvrRps4 interaction with the WRKY domain disrupts WRKY–domain 4 association, thus derepressing the complex. PopP2-triggered activation is less easily explained by such disruption and involves the longer C-terminal extension of RRS1-R. Furthermore, some mutations in RPS4 and RRS1 compromise PopP2 but not AvrRps4 recognition, suggesting that AvrRps4 and PopP2 derepress the complex differently. Consistent with this, a "reversibly closed" conformation of RRS1-R, engineered in a method exploiting the high affinity of colicin E9 and Im9 domains, reversibly loses AvrRps4, but not PopP2 responsiveness. Following RRS1 derepression, interactions between domain 4 and the RPS4 C-terminal domain likely contribute to activation. Simultaneous relief of autoinhibition and activation may contribute to defense activation in many immune receptors.

paired NLR immune receptors | effector-triggered immunity | integrated decoy | effector target | plant-disease resistance

Plants and animals carry both intracellular and cell-surface localized immune receptors that activate defense upon recognition of molecules from pathogens. Plant transmembrane receptors recognize extracellular microbial molecules and activate pattern-triggered immunity. Pathogen effector proteins suppress immunity and promote pathogen virulence, but plant intracellular immune receptors can recognize intracellular effectors, either directly or indirectly (1, 2). Genetic variation for disease resistance usually maps to genes that encode intracellular receptors that are modular nucleotide-binding (NB) leucine-rich repeat (LRR) proteins, termed NLRs, that resemble animal NOD-like immune receptors (3, 4). Plant NLRs usually carry either an N-terminal Toll–interleukin-1 receptor/resistance protein (TIR) domain or an N-terminal coiled-coil (CC) domain (5). Recognition of effectors by NLRs leads to effector-triggered immunity, often culminating in a hypersensitive cell death response (HR).

How plant NLR proteins function remains unclear. The NB domain may act as molecular switch driven by ATP or ADP binding, which, upon effector recognition, may change conformation to stabilize the ATP-bound form of the NLR, leading to activation (6–9). TIR domains of many TIR-NLRs such as flax L6

and *Arabidopsis* RPP1 and RPS4 are sufficient to activate defense signaling when overexpressed (10–14). Allelic variation for recognition in NLRs usually maps to the LRR domain (15). Effector–LRR interaction might relieve autoinhibitory intramolecular interactions, enabling activation of the N-terminal signaling domain (16).

## Significance

Plants and animals carry intracellular nucleotide-binding leucine-rich repeat (NLR) immune receptors. How NLR receptors activate defense on perceiving pathogen molecules is poorly understood, especially in plants. Some NLRs function in pairs, with one NLR carrying a domain that mimics a pathogen effector target. Effector action on this domain activates the second "helper" NLR. In the *Arabidopsis* RPS4 and RRS1 pair, RRS1 carries a WRKY transcription factor domain targeted by bacterial effectors AvrRps4 and PopP2. We monitored conformational changes in RPS4–RRS1 during activation and developed a "molecular padlock" to reversibly restrict such changes. This revealed domains within RRS1 required to keep the RRS1–RPS4 complex inactive prior to effector detection, and specific domain–domain interactions whose disruption or modification contributes to defense activation.

Some NLRs function in pairs (17, 18), each of which specializes into sensor or executor (or "helper") roles for effector perception and immune signaling. The sensor NLR can detect effectors via an integrated domain (ID) that mimics an authentic pathogen target (19, 20). Genetically linked sensor and executor NLR pairs, such as rice RGA4 and RGA5 and *Arabidopsis* RRS1 and RPS4, form immune complexes in which the sensor NLR carrying an ID (RGA5, RRS1) detects effectors, and helper NLR (RGA4, RPS4) activates defense (3, 21). The sensors RRS1 and RGA5 negatively regulate their cognate executors RPS4 and RGA4 (17, 22). Some sensor NLRs require unlinked "helper NLRs" to activate signaling (18, 23–25). Failure to appropriately interact with partners can result in loss of defense activation or autoactivity (26–28).

How paired immune receptor complexes convert effector sensing into defense activation is unknown. *RRS1-R* encodes a TIR-NLR (TNL) protein with a WRKY domain near the C terminus. WRKY transcription factors are key regulators of plant defense. RRS1-R from accessions Ws-2 forms an immune receptor complex with RPS4 that recognizes AvrRps4 from *Pseudomonas syringae* and PopP2 from *Ralstonia solanacearum* (29–31). AvrRps4 and PopP2 target a subset of host WRKY proteins to suppress host defense and promote pathogen virulence. Both effectors are perceived via the integrated WRKY domain of RRS1-R. AvrRps4 interacts with, and PopP2 acetylates, the WRKY domain, resulting in activation of the RPS4–RRS1 complex and subsequent defense activation (32, 33). RRS1 thus monitors for effectors that target WRKY proteins. *Arabidopsis* accessions also carry an NLR pair RRS1B/RPS4B (sharing ~70% identity with and closely linked to RRS1/RPS4) that detects AvrRps4, but not PopP2 (26). PopP2 is not recognized by RRS1-S/RPS4 from the *Arabidopsis* accession Col-0, likely due to a truncation of the C-terminal extension beyond the WRKY domain in RRS1-R (33). Since RRS1-S/RPS4 is fully responsive to AvrRps4, PopP2 might activate the immune complex differently from AvrRps4.

How do immune complex reconfigurations convert effector sensing into defense activation? We found that the integrated WRKY domain of RRS1 negatively regulates the immune receptor complex, and effector interactions with the WRKY domain abrogate its negative regulation. RRS1-R engineered with a "reversibly closed" conformation exhibits reversible loss of AvrRps4, but not PopP2 recognition. We infer substantial rearrangements of the C-terminal domains (CTDs) of RRS1-R are required during AvrRps4 responsiveness, while more subtle changes are involved in PopP2 responsiveness. Genetic evidence suggests the post-LRR CTD of RPS4 is required for subsequent signaling, with some amino acids required for PopP2 but not AvrRps4 responsiveness. This combination of relief of autoinhibition and activation will likely operate in many other immune receptor systems.

## Results

### RRS1 WRKY Domain (DOM5) Is Required for Autoinhibition, and Domain 4 (DOM4) for Activation of the RRS1–RPS4 Complex.
We tested the role of the WRKY domain of RRS1 in regulating the RRS1–RPS4 complex in the absence of effector. RRS1-R mutations in the WRKY domain constitutively activate defense [e.g., sensitive to low humidity 1 (*slh1*) and *K1221Q*] or block signaling (e.g., *K1221R*) (33, 34). As the loss of DNA binding by RRS1-S$^{slh1}$ or RRS1-R$^{K1221R}$ is insufficient to trigger activation (32, 33), DNA binding by the WRKY domain, or its loss, is unlikely to directly activate defense. We hypothesized that, after interaction with an effector, the WRKY domain initiates conformational changes in RRS1 domains that are sensed by RPS4, activating defense.

For RRS1, we defined the 322 aa between the LRRs and WRKY as domain 4 (DOM4 or D4) and the amino acids C-terminal to the WRKY domain as domain 6 (DOM6-R is 104 aa,

DOM6-S is 21 aa) (*SI Appendix*, Fig. S1*A*). *RPS4* encodes a TNL with 338 aa C-terminal to the LRR, designated here the CTD (*SI Appendix*, Fig. S1*A*). These domain boundaries were defined to minimize potential disruption during domain swaps. For simplicity, chimera proteins are represented with domains from RRS1 and RPS4 as A's, and domains from RRS1B and RPS4B as B's.

To investigate the roles of DOM6, WRKY, and DOM4, we made several C-terminal deletions of RRS1-R and analyzed function using transient assays in *Nicotiana tabacum* (tobacco) leaves. We confirmed that deleting 83 aa of RRS1-R (ΔC83) abolishes PopP2 but not AvrRps4 recognition when coexpressed with RPS4, phenocopying RRS1-S (Fig. 1*A*). Similarly, RRS1-RΔC101, in which all but 3 aa of DOM6-R are deleted, responds to AvrRps4 and is not constitutively active (Fig. 1*A*). Thus, DOM6-R of RRS1-R is dispensable for AvrRps4 recognition but is essential for converting PopP2 acetylation of the WRKY domain into defense activation.

Notably, further deletion to remove the WRKY domain (DOM5), making RRS1-RΔD56 (lacking domains 5 and 6), results in constitutive RPS4-dependent activity (Fig. 1*A*). Domain swaps in which the RRS1-R WRKY domain was replaced with a bacterial LexA DNA binding domain (33), or with the RRS1B WRKY domain (56.6% amino acid identity), also show RPS4-dependent autoactivity (Fig. 1*B*). Unlike the inactive RRS1-S$^{slh1}$ (33), RRS1-S(AAAALA) with the WRKY replaced by LexA (L), also shows RPS4-dependent constitutive activity (Fig. 1*B*). Thus, removal or perturbation of the WRKY domain is sufficient to activate defense, implying that it acts as a negative regulator of the immune complex, rather than in downstream signaling. Intriguingly, substituting DOM6 of RRS1 with that of RRS1B leads to autoactivity of RRS1(AAAAAB), while deletion of DOM6 in RRS1 does not (Fig. 1 *A* and *B*). Therefore, this constitutive activity is likely caused by the presence of an incompatible DOM6-B, rather than by the lack of DOM6-R. Replacing DOM5 and DOM6 with the equivalent domains from RRS1B [to make RRS1-R(AAAABB)], or with the WRKY domain and C-terminal amino acids from WRKY41 [RRS1-R (AAAAW41)], also results in autoactivity (Fig. 1*B* and *SI Appendix*, Fig. S1*B*). WRKY41 is closely related to both RRS1 and RRS1B WRKY domains (*SI Appendix*, Fig. S1*B*) and interacts with AvrRps4 and PopP2 (33), suggesting that WRKY41 may represent the original effector target from which these integrated WRKY domains evolved. We hypothesize that the WRKY domains of RRS1B and WRKY41 fail to suppress DOM4 of RRS1 in RRS1-R(AAAABB) and RRS1-R(AAAAW41), thus allowing RRS1-R to activate RPS4. Reciprocal DOM5 and/or DOM6 swaps in RRS1B all lead to RPS4B-dependent autoactivity (*SI Appendix*, Fig. S1*C*), suggesting that compatible interactions between WRKY and its adjacent domains are important for autoinhibition in both the A and B pair complexes. This also indicates that IDs must coevolve with the main body of the NLR receptors after fusion.

The autoactivity of RRS1-RΔD56 requires DOM4 of RRS1-R, since deletion of DOM4 abolishes RRS1-RΔD456 autoactivity and effector responsiveness (Fig. 1*A*). The importance of DOM4 for activation is also shown by DOM4 swaps. Both RRS1 (AAABAA) + RPS4 and RRS1B(BBBABB) + RPS4B combinations fail to respond to effectors (Fig. 1*C* and *SI Appendix*, Fig. S2*B*). Swapping NB-ARC or LRR domains of RRS1 with RRS1B abrogates effector responsiveness of RRS1(ABAAAA) and RRS1(AABAAA) without causing autoactivity (Fig. 1*C*), suggesting that matching NB-ARC and LRR domains are required for complex activation. *SI Appendix*, Fig. S1*A* illustrates the domain boundaries for swapping and deletion experiments. Lack of effector responsiveness is not due to the lack of R protein expression (*SI Appendix*, Fig. S1*D*).
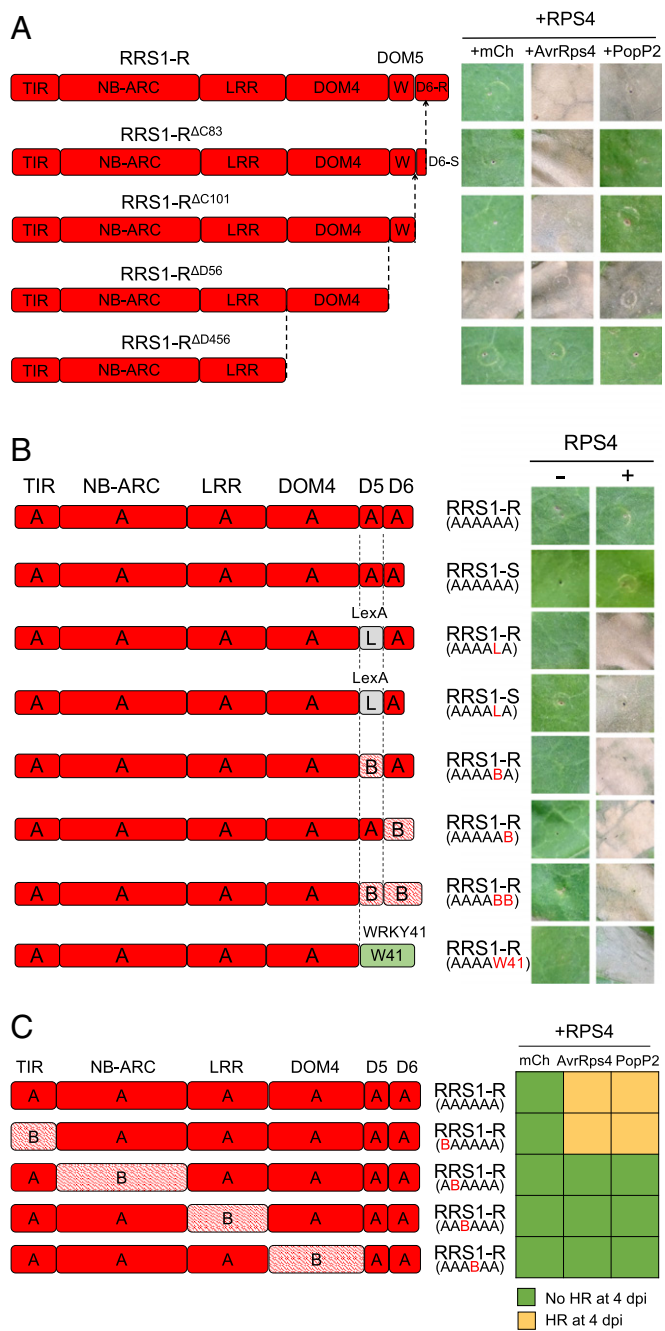
**Fig. 1.** RRS1 WRKY domain (DOM5) is required for autoinhibition and domain 4 (DOM4) for activation of the RRS1–RPS4 complex. (A) Successive deletions of RRS1-R compromise effector responsiveness or autoinhibition. Each tobacco leaf section was coinfiltrated to transiently express RPS4 and a truncated RRS1-R with either mCherry (mCh), AvrRps4:mCh or PopP2:mCh. ΔC83, deletion of C-terminal 83 aa of RRS1-R; ΔD56, deletion of the WRKY domain (DOM5) and domain 6 of RRS1-R (DOM6-R). (B) Replacement of DOM5 and/or DOM6 of RRS1 with that of RRS1B causes RPS4-dependent autoactivity. Each leaf section was infiltrated to express a chimeric RRS1 with or without RPS4. The chimeras are represented with domains from RRS1 as A's, domains from RRS1B as B's, bacterial LexA shown as L, and the WRKY domain and C-terminal amino acids of WRKY41 shown as W41. (C) Loss of effector responsiveness in the RRS1-R chimeras where NB-ARC, LRR, or domain 4 (DOM4) is replaced by an equivalent domain of RRS1B, when coexpressed with RPS4. Each section represents the presence (yellow) or absence (green) of HR in tobacco leaves at 4 d postinfiltration (dpi). HRs were assessed at 4 dpi. Phenotypes are representative of at least three consistent replicates.

To test whether the expressed subdomain D56-R (DOM5 + DOM6-R) associates with other domains of RRS1 to suppress activation, we carried out coimmunoprecipitation (co-IP) experiments after transient coexpression in *Nicotiana benthamiana* (*Nb*) leaves. D56-R coimmunoprecipitates more strongly with expressed subdomain 4 (DOM4) than with NB-ARC or LRR of RRS1, indicating that D56-R association with DOM4 could be responsible for the negative regulation of the RRS1–RPS4 complex (*SI Appendix*, Fig. S1E). Nevertheless, *in trans* coexpression of D56-R cannot suppress RRS1-RΔD56 + RPS4-triggered HR (*SI Appendix*, Fig. S1F), suggesting that D56-R must be in the context of full-length RRS1-R for autoinhibition. Similarly, *in trans* coexpression of DOM4 and RRS1-RΔD456 cannot reconstitute the autoactivity of RRS1-RΔD56 + RPS4, and RRS1-RΔD456 + D456-R is nonresponsive to AvrRps4 (*SI Appendix*, Fig. S1F). These data suggest intramolecular interactions between domains of RRS1 are required for autoinhibition and activation of the immune complex.

**Distinct Genetic Requirements in RPS4 and RRS1 for PopP2 and AvrRps4 Responsiveness, and for Autoactivity.** RRS1-RΔD56 requires a signaling-competent RPS4 to trigger cell death. The RPS4 P-loop mutant RPS4(K242A) or TIR domain mutant RPS4(SHAA) (13) fail to activate HR when coexpressed with RRS1-RΔD56 (*SI Appendix*, Fig. S2A). In contrast, the P-loop mutant of RRS1-RΔD56(K185A) still activates RPS4-dependent HR (*SI Appendix*, Fig. S2A).

Upon derepression, RRS1 signals via RPS4. Either truncation of RPS4 CTD, or a CTD swap with RPS4B [RPS4(AAAB)], or several point mutations in the CTD (C887Y, S914F, G952E, G997E), impair RPS4 + RRS1-RΔD56–triggered HR (Fig. 2A). These point mutations were found in a genetic screen (34). Compared with C887Y and S914F, mutations G952E and G997E of RPS4 show a stronger impairment (Fig. 2A). These data suggest that the CTD is essential for RPS4 to respond to a derepressed RRS1-RΔD56, possibly via DOM4.

Using domain swaps, we tested whether the cognate DOM4 and CTD from RRS1-R/RPS4 (A pair) or RRS1B/RPS4B (B pair) are required for effector-triggered activation. DOM4 swaps between RRS1-R and RRS1B result in no response to AvrRps4 and PopP2 when coexpressed with their cognate pair partners (Fig. 2B and *SI Appendix*, Fig. S2B). After swapping the CTD, RPS4B(BBBA) + RRS1B fails to respond to either effector, while RPS4(AAAB) + RRS1-R recognizes both AvrRps4 and PopP2 (Fig. 2B and *SI Appendix*, Fig. S2B). Since RPS4(AAAB) + RRS1-RΔD56 fail to trigger cell death (Fig. 2A), the presence of D56 in RRS1-R compared with RRS1-RΔD56 must explain this contrast in functionality (Fig. 2 G and H). RPS4 and RPS4B chimeras express at levels comparable to wild type (*SI Appendix*, Fig. S2D). These data suggest that DOM4 and CTD complementarity is important for effector responsiveness. However, even when DOM4 and CTD are from matching pairs [RRS1-R(AAABAA) + RPS4(AAAB); RRS1B(BBBABB) + RPS4B(BBBA)], the effector responsiveness is lost (Fig. 2B and *SI Appendix*, Fig. S2B), indicating that a matching DOM4/CTD is not sufficient for function.

We next examined previously identified RRS1 DOM4 and RPS4 CTD mutants (34) for effector responsiveness in transient assays. When coexpressed with RPS4, RRS1-R DOM4 mutants S983F and E1070K both show reduced PopP2 but full AvrRps4 responsiveness (Fig. 2C). When the RPS4 CTD mutant C887Y is coexpressed with RRS1-R, it also shows partial loss of PopP2, but not of AvrRps4, responsiveness (Fig. 2D). Quantification confirms the stronger impairment of PopP2 compared with AvrRps4 responsiveness for these mutants (Fig. 2F). Other RPS4 CTD mutants tested (S914F, G952E, G997E) lose recognition of both effectors in combination with RRS1-R, suggesting that these residues are necessary for activation triggered by either effector (34) (*SI Appendix*, Fig. S2C). Some residues in DOM4 and CTD
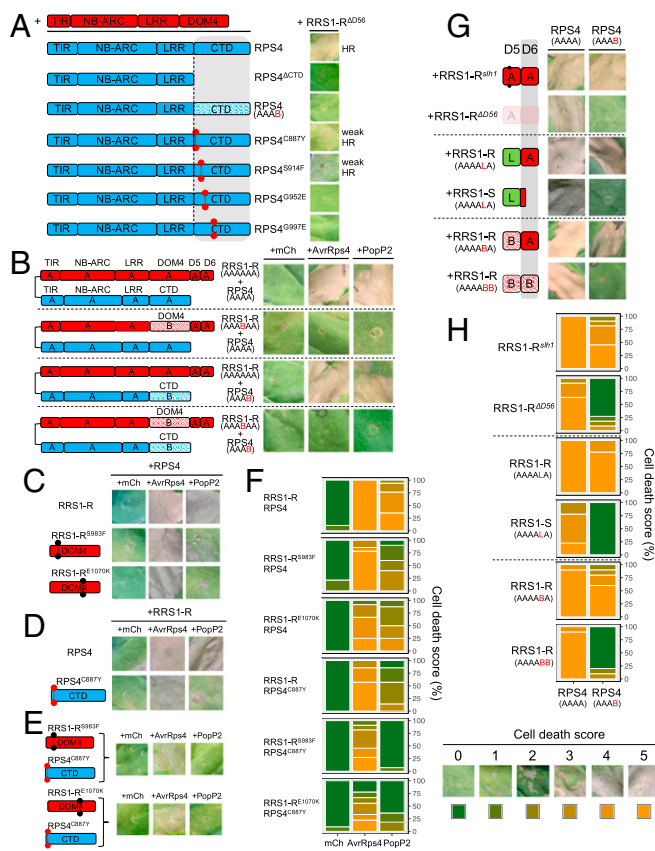
Ma et al.

**Fig. 2.** Distinct genetic requirements in RPS4 and RRS1 for PopP2 and AvrRps4 responsiveness, and for autoactivity. (*A*) RPS4 C-terminal domain (CTD) is required for RPS4 + RRS1-RΔD56–triggered HR. Each leaf section was coinfiltrated to express RRS1-RΔD56 with a CTD variant of RPS4. Deletion of CTD (ΔCTD), CTD swap with RPS4B [RPS4(AAAB)], or several mutations in CTD (C887Y, S914F, G952E, G997E) impair the HR activity of RPS4 + RRS1-RΔD56. (*B*) DOM4 swap with RRS1B and/or CTD swap with RPS4B influence effector responsiveness of RRS1-R/RPS4. Each leaf section was coinfiltrated to express wild-type or chimeric RRS1-R and RPS4 with mCh, AvrRps4, or PopP2. (*C–E*) Mutations S983F, E1070K in RRS1-R DOM4, and C887Y in RPS4 CTD primarily impair PopP2-, but not AvrRps4-triggered HR. Each leaf section was coinfiltrated to express wild-type or mutant RRS1-R, RPS4 with mCh, AvrRps4, or PopP2. (*G*) DOM6 of RRS1-R is required to compensate for the noncognate RRS1 DOM4(A) and RPS4B CTD(B) combination. Each leaf section was coinfiltrated to express either RPS4 or RPS4(AAAB) with an autoactive RRS1 variant. Only the RRS1 variants possessing a DOM6-R trigger HR with RPS4(AAAB). For *A–E* and *G*, HRs were assessed at 4 dpi. Photographs are representative of three consistent replicates. (*F* and *H*) Percentage representations of cell death scores in *C–H* at 4 dpi. Stacked bars are color-coded to show the proportions (in percentage) of each cell death scale (0–5) out of the total infiltrated panels scored. Panel (0) in cell death score is reused from the second row of *G*. Total panels scored are 7–19 (*F*) and 9–11 (*H*).

are thus more important for PopP2- than for AvrRps4-triggered activation. We hypothesize that these residues are in a unique DOM4–CTD interaction interface that participates in PopP2-triggered activation, likely involving RRS1-R domain 6 (DOM6-R). Consistent with this idea, this partial PopP2 responsiveness is further decreased when the two mutants are combined in RRS1-R$^{S983F}$ + RPS4$^{C887Y}$, or RRS1-R$^{E1070K}$ + RPS4$^{C887Y}$ (Fig. 2 *E* and *F*). Importantly, these combinations can still recognize AvrRps4, albeit showing weaker HR (Fig. 2 *E* and *F*). We therefore infer that these residues of DOM4 (S983, E1070) and CTD (C887) may cooperate to enable PopP2-triggered complex activation via a mechanism that is not required for AvrRps4 responsiveness.

DOM6-R is specifically required for PopP2 but not AvrRps4 recognition (Fig. 1*A*). D56-R enables complex activation even in a noncognate DOM4(A)/CTD(B) combination; RRS1-R + RPS4 (AAAB) confers responsiveness to both effectors, whereas RRS1-RΔD56 + RPS4(AAAB) fail to trigger HR (Fig. 2 *A* and *B*). Additionally, RRS1-R$^{slh1}$ + RPS4(AAAB) trigger HR, suggesting that D56-R$^{slh1}$ promotes activation despite a noncognate DOM4(A), CTD(B) combination (Fig. 2 *G* and *H*). To test whether DOM6-R alone enables this activity, we compared WRKY substitutions by LexA in RRS1-R and RRS1-S, and also RRS1(AAAABA) and RRS1(AAAABB) for their activities with RPS4(AAAB). Although all RRS1 chimeras coexpressed with RPS4 are autoactive, only RRS1-R(AAAALA) and RRS1-R(AAAABA) with a DOM6-R trigger HR with RPS4(AAAB) (Fig. 2 *G* and *H*). In contrast, RRS1-S(AAAALA) with DOM6-S and RRS1-R(AAAABB) with DOM6-B exhibit no or weak HR in the presence of RPS4(AAAB), suggesting that DOM6-R is specifically required to function with RPS4(AAAB) (Fig. 2 *G* and *H*). Since DOM6-R is able to compensate for a DOM4–CTD mismatch, it may promote activation via assisting or modulating DOM4–CTD association.

In summary, we identified distinct genetic requirements in RPS4 and RRS1 for PopP2 and AvrRps4 responsiveness. DOM6-R enables PopP2-triggered activation of the complex, possibly by modulating interactions between DOM4 and CTD or DOM4 and WRKY domain.

**Interactions Between DOM4 and D56 of RRS1 Are Influenced by Effectors, Mutations, and Domain Swaps That Activate the Complex.** We hypothesized that the WRKY domain (DOM5) negatively regulates the RRS1–RPS4 complex preactivation, and that during effector-imposed alleviation of that negative regulation, DOM4 plays a role in activating the complex. We found that for RRS1-R domains, DOM4(A) coimmunoprecipitates with D56-R (AA), and DOM4(A) coimmunoprecipitates more strongly with DOM5(A) than with DOM6-R(A) (Fig. 3*A*). This suggests that, in RRS1-R, DOM4–D56-R association is mainly via the WRKY domain and that the DOM4–WRKY interaction likely inhibits the complex. In contrast, D56(BB) of RRS1B fails to coimmunoprecipitate with DOM4(A) of RRS1, and DOM5(B) coimmunoprecipitates less than DOM5(A) with DOM4(A) (Fig. 3*A*). The autoactivity of RRS1-R(AAAABB) and RRS1-R(AAAABA) might arise because D56(BB) or DOM5(B) fails to impose a strong negative regulation on DOM4(A), derepressing RRS1, as does deletion of D56-R in RRS1-RΔD56.

We next tested whether the autoactivity of several RRS1-R WRKY domain mutants correlates with lack of D56–DOM4 interactions. We assessed interactions of RRS1-R DOM4 with D56-R carrying autoactive mutations *slh1* or *K1221Q* (*K2Q*), or a nonautoactive mutation *K1221R* (*K2R*), and found that all D56-R mutants coimmunoprecipitate with DOM4 (Fig. 3*B*). Compared with D56-R and D56-R$^{K2R}$ (lanes 1 and 3), DOM4 coimmunoprecipitates less with D56-R$^{slh1}$ and D56-R$^{K2Q}$ (lanes 2 and 4) (Fig. 3*B*). However, as these autoactive D56-R forms show lower levels in the input, it is difficult to quantitatively compare their strength of interactions. In addition, D56-S from RRS1-S, with an identical DOM5 to RRS1-R and a shorter DOM6-S, also show lower levels in the input and coimmunoprecipitates less with DOM4 (lane 5) than D56-R (Fig. 3*B*).

These data suggest that RRS1 autoactive forms can promote defense without abolition of DOM4/D56 affinity. Conceivably, certain mutations in the WRKY domain can cause a change in the DOM4/D56 conformation that is not reflected by affinity differences in co-IP assays, but is sufficient to derepress RRS1-R. Interestingly, DOM4(B) coimmunoprecipitates with both D56(AA) and DOM5(A), but with no or weaker affinity to D56(BB) and DOM5(B) (*SI Appendix*, Fig. S3*A*), suggesting that mechanisms of autoinhibition might differ between RRS1 and RRS1B.
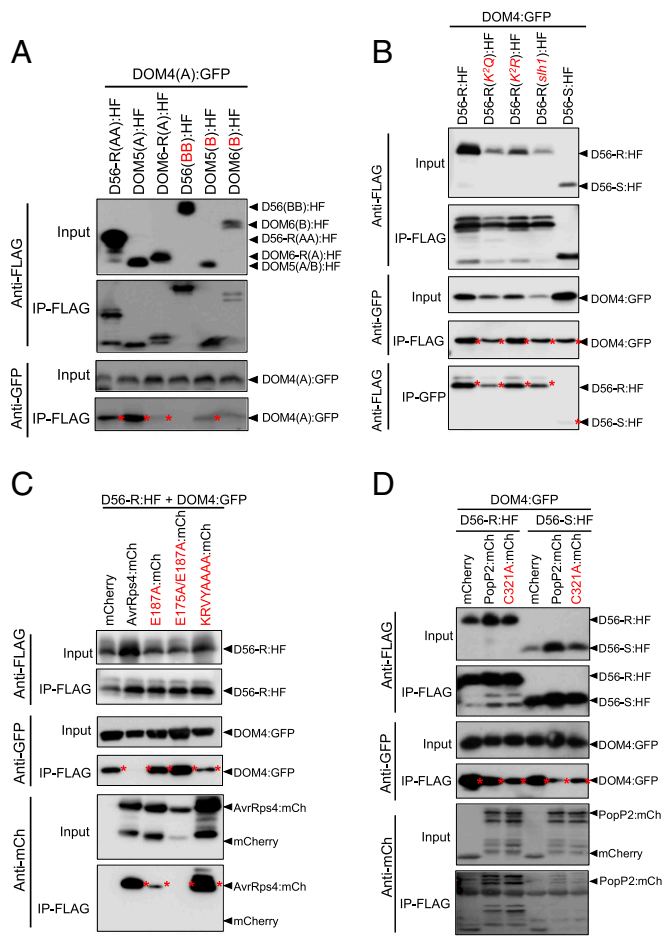
**Fig. 3.** Interactions between DOM4 and D56 of RRS1 are influenced by effectors, mutations and domain swaps that activate the complex. (A) Co-IP assays to assess RRS1-R DOM4(A):GFP association with HF-tagged D56, DOM5, and DOM6-R of RRS1-R (A) and RRS1B (B) after transient coexpression in *Nb* leaves. DOM4(A) coimmunoprecipitates more strongly with A compared with B domains. (B) Co-IP assays to assess RRS1-R DOM4:GFP association with different alleles or mutants of D56:HF. D56-R and D56-S are of RRS1-R and RRS1-S, respectively. *K2Q* and *K2R* are acetyl-mimic and acetyl-null mutations of *K1221* in RRS1-R WRKY domain. *slh1* is a leucine insertion in RRS1-R WRKY domain. (C and D) Co-IP assays reveal effector interference with DOM4:GFP–D56-R:HF or DOM4:GFP–D56-S:HF association. Effectors are tagged with mCherry (mCh). Controls include AvrRps4 mutants E187A, E187A/E175A (EEAA) and KRVYAAAA (KRVY), a PopP2 mutant C321A, and mCherry. AvrRps4 inhibits DOM4–D56-R association, and PopP2 weakly interferes with both DOM4–D56-R and DOM4–D56-S association. Immunoblots show protein accumulations in total extracts (input) and after IP with anti-FLAG(IP-FLAG) or anti-GFP(IP-GFP) beads. Asterisks mark bands that indicate (lack of) associations. These were repeated three times with similar results.

AvrRps4 and PopP2 are detected by the WRKY domain of RRS1. We hypothesized that effector engagement with the WRKY domain derepresses RRS1 by interfering with interactions between DOM4 and D56. AvrRps4 inhibits DOM4–D56-R interactions in co-IP assays (Fig. 3C). We mutated residues (E187, E175) of AvrRps4 reported previously to be important for recognition (35) and verified that both AvrRps4-E187A and the E187A/E175A (hence, AvrRps4-EEAA) lose recognition by RRS1-R/RPS4 (*SI Appendix*, Fig. S3B). Importantly, AvrRps4 E187A and EEAA, which exhibit weak and no affinity to D56-R, respectively, show reduced or no interference with DOM4–D56-R association (Fig. 3C). In contrast, although not recognized, AvrRps4-KRVYAAAA (AvrRps4-KRVY) can interfere with DOM4–D56-R associations, although less than AvrRps4. This is

consistent with the strong affinity observed between AvrRps4-KRVY and D56-R (Fig. 3C). These data suggest that AvrRps4 derepresses RRS1 via disrupting DOM4–D56 associations, and inadequate disruption by E187A and EEAA mutants explains their inability to activate RRS1-R/RPS4. On the other hand, AvrRps4-KRVY suppresses DOM4–D56 association, indicating that reducing DOM4–D56 association is not sufficient to activate defense.

PopP2 shows a weaker interference of DOM4–D56-R association compared with AvrRps4 (Fig. 3D). Consistently, D56-R$^{K2Q}$ (*K1221Q*), which mimics PopP2 acetylation of the WRKY domain residue K1221, does not show complete loss of association with DOM4 (Fig. 3B). PopP2 also suppresses DOM4–D56-S association (Fig. 3D), even though RRS1-S cannot activate defense in response to PopP2. The enzymatically inactive mutant PopP2-C321A exhibits moderate suppression of both DOM4–D56-R and DOM4–D56-S associations, resembling the effect of PopP2 (Fig. 3D and *SI Appendix*, Fig. S3B). Overall, PopP2 acetylation of the WRKY domain may not lead to complete dissociation of DOM4–D56-R, and PopP2 likely activates the complex differently than AvrRps4.

### RPS4 CTD Interacts with RRS1 D456, but Changes in RPS4 CTD–D456 Affinity Do Not Explain the Difference Between Inactive and Activated Forms of the Complex.

We investigated interactions of CTD with domains 4, 5, and 6 of RRS1 and found that RPS4 CTD associates with RRS1 DOM4 (Fig. 4A). We hypothesized that this association might be important for signal transduction between the sensor (RRS1) and the executor (RPS4) and tested whether mutations or domain swaps that compromise signaling also impair their interactions. DOM4(RRS1) coimmunoprecipitates with both CTD(RPS4) and CTD(RPS4B). However, cognate pairs [DOM4(A)–CTD(A); DOM4(B)–CTD(B)] did not show stronger affinity than the noncognate pairs [DOM4(B)–CTD(A); DOM4(A)–CTD(B)] (*SI Appendix*, Fig. S4A). Similarly, associations between mutants of DOM4 or CTD are unaltered in co-IP (*SI Appendix*, Fig. S4B).

The RPS4 CTD coimmunoprecipitates more strongly with D456-R than with DOM4 but does not associate with D56-R (Fig. 4 A and B), suggesting that CTD and DOM4 interactions
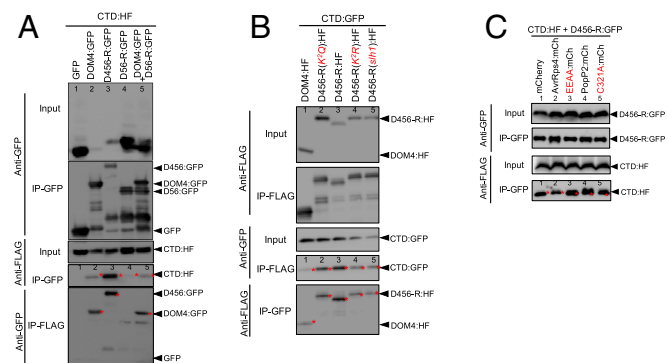


**Fig. 4.** Interactions between RPS4 CTD and RRS1 D456 are influenced by effectors and mutations that activate the complex. (A) Co-IP assays to assess RPS4 CTD:HF association with GFP-tagged DOM4, D56-R, D456-R of RRS1-R after coexpression in *Nb* leaves. CTD coimmunoprecipitates strongly with D456-R and more weakly with DOM4, but not with D56-R. (B) Co-IP assays to show RPS4 CTD:GFP association with mutants of D456-R:HF (*K2Q*, *K2R*, *slh1*). CTD coimmunoprecipitates more weakly with these mutants than with D456-R. (C) Co-IP assays reveal effector interference of RPS4 CTD:GFP and RRS1-R D456-R:HF associations. Effectors are tagged with mCh. Controls include AvrRps4 mutant EEAA, PopP2 mutant C321A, and mCherry. AvrRps4 but not PopP2 interferes with CTD–456-R associations. Immunoblots show protein accumulation in input and after IP-FLAG or IP-GFP. Asterisks mark bands that indicate association. These were repeated three times with similar results.

are likely modulated by D56-R. However, coexpression *in trans* of D56-R with DOM4 does not alter DOM4–CTD association affinity (lanes 2 and 5) (Fig. 4*A*). D56-R might enhance D456-R's affinity with CTD *in cis*, which could change upon mutation- or effector-triggered derepression. We tested the affinity of several D456-R mutants (*K2Q*, *K2R*, *slh1*) with CTD, and our data suggest that all mutants coimmunoprecipitate more weakly than wild type (lane 3) with CTD (Fig. 4*B*). We also found that AvrRps4, but not EEAA, slightly reduces D456-R–CTD association by co-IP in both directions (Fig. 4*C* and *SI Appendix*, Fig. S4*C*), suggesting that a derepressed D456-R has reduced affinity with RPS4 CTD. However, PopP2 or PopP2-C321A do not suppress D456-R–CTD association (Fig. 4*C*). As PopP2 shows a weaker interference of DOM4–D56-R association compared with AvrRps4 (Fig. 3 *C* and *D*), it is likely that PopP2 derepresses D456-R differently, which alters D456-R's association with RPS4 CTD to activate defense without reducing their affinity.

In summary, RPS4 CTD associates with RRS1 D456, likely via interactions with DOM4 that are potentiated by DOM56. However, the mechanism of RPS4 activation by activated RRS1 cannot be explained by changes in the presence or absence of CTD–DOM4 interactions.

**Bimolecular Fluorescence Complementation Analyses Reveal Effector-Dependent Conformational Differences in RRS1 D456.** Genetic and biochemical data above highlight the importance of RRS1 D456 during autoinhibition and activation of the immune complex. We investigated preactivation and postactivation conformational differences of D456 using bimolecular fluorescence complementation (BiFC). We visualized DOM4–D56-R associations using cCFP:D456-R:nVenus (Fig. 5*E* and *SI Appendix*, Fig. S5*H*) or cCFP:D456-R:nCerulean (nCer) (*SI Appendix*, Fig. S5*D*),

which show strong BiFC signals (YFP and CFP, respectively) in nuclei after transient expression in *Nb* leaves, as does cCFP:D456-S:nVenus (Fig. 5*E*). Assuming that intramolecular interactions within D456 give rise to these BiFC signals, these results suggest a "closed" D456 conformation preactivation, with N and C termini of RRS1 D456 in close proximity. As D456-R self-associates in co-IP assays (*SI Appendix*, Fig. S5 *A* and *B*), it is also possible that these signals are produced intermolecularly, meaning that N terminus (DOM4) of one molecule could associate with C terminus (DOM6) of another. In one such scenario, two linear D456 molecules associate in an antiparallel manner ("open" model), and the N and C termini of D456 would not be in close proximity, contrary to the anticipated closed model (*SI Appendix*, Fig. S5*C*). To distinguish these scenarios, we tested the combinations cCFP:D456-R + nCer:D456-R (N + N), D456-R:cCFP + D456-R:nCer (C + C), and cCFP:D456-R + D456-R:nCer (N + C). All combinations (N + N, C + C, N + C) produce significantly weaker BiFC signals compared with cCFP:D456-R:nCer, favoring the closed model (*SI Appendix*, Fig. S5 *D* and *E*). Furthermore, the higher signal intensities shown for cCFP:D456-R:nCer (*SI Appendix*, Fig. S5 *D* and *E*), strongly suggest that intramolecular rather than intermolecular interactions contribute to its BiFC signal. These data suggest that, in the absence of effector, the N and C termini of D456 are in close proximity.

We set out to assess changes in D456 in the context of full-length RRS1, as D456-R cannot activate RPS4 upon effector treatment (*SI Appendix*, Fig. S5*F*). We generated RRS1-R (cCFP-nVenus), carrying a cCFP between LRR and DOM4 and an nVenus at the C-terminal end. Importantly, RRS1-R(cCFP-nVenus) can respond to AvrRps4, but not to PopP2, when coexpressed with RPS4, albeit more weakly than RRS1-R:HF ($6\times$His$3\times$FLAG) (Fig. 5*A*). RRS1-R(cCFP-nVenus) exhibits
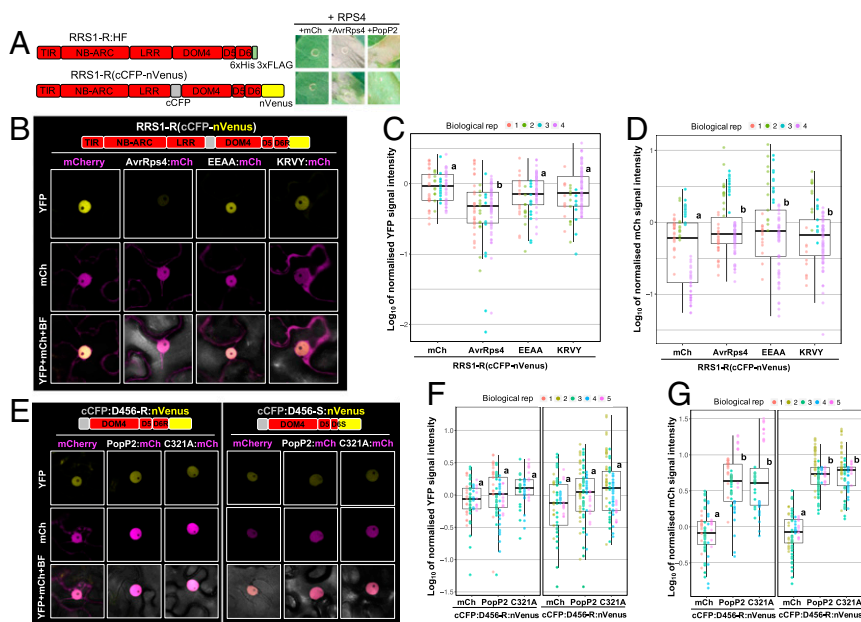


**Fig. 5.** BiFC analyses reveal effector-dependent conformational differences in RRS1 D456. (*A*) RRS1-R(cCFP-nVenus) + RPS4 respond to AvrRps4 (weaker than RRS1-R:HF + RPS4), but not PopP2, in tobacco transient assays. Diagram of RRS1-R(cCFP-nVenus) illustrates a cCFP between LRR and DOM4, and an nVenus at the C terminus. HRs were assessed at 3 dpi. Photographs are representative of three consistent replicates. (*B–D*) Nuclear BiFC signal of RRS1-R(cCFP-nVenus) is reduced in the presence of AvrRps4:mCh, but not AvrRps4 mutants, after coexpression in *Nb* leaves at 2 dpi. Representative images are shown (*B*). Box plots show quantifications of YFP signals (*C*) and mCh signals (*D*). (*E–G*) Nuclear BiFC signals of cCFP:D456-R:nVenus or cCFP:D456-S:nVenus remain unaltered in the presence of PopP2:mCh or C321A:mCh, compared with mCherry control. Representative images are shown (*E*). Box plots show quantifications of YFP signals (*F*) and mCh signals (*G*). Signal intensity of YFP (*B* and *F*) or mCh (*C* and *G*) was quantified as average gray value of each nucleus, and then each normalized to the mean intensity (YFP or mCh) of the mCh control sample within each biological replicate. Data points, color-coded for different biological replicates, represent Log$_{10}$ of the normalized values. Linear mixed-effects model (lme) and tests for general linear hypotheses (glht) with Tukey comparisons were used for statistical analysis. Means with the same letter are not significantly different ($P < 0.001$).

strong BiFC signals in the absence of effectors (Fig. 5B). Conceivably, the affinity of cCFP for nVenus partially compromises functionality of the RRS1–RPS4 complex. This suggests that preactivation, the N terminus of DOM4 is close to the C terminus of DOM6-R in full-length RRS1-R, forming a closed D456-R. AvrRps4 interferes with the BiFC signal of RRS1-R (cCFP-nVenus), whereas neither mutant (EEAA nor KRVY) significantly alters this BiFC signal compared with the mCherry (mCh) control (Fig. 5 B and C) despite comparable expression levels (Fig. 5D). We quantified BiFC signal intensity in each nucleus, and then normalized to the average value of RRS1-R (cCFP-nVenus) + mCh to compare different effector treatments, enabling evaluation of statistical significance in BiFC differences (Fig. 5C and *SI Appendix*, Table S2). Similarly, quantification of mCherry signals was used to compare effector expression levels (Fig. 5D). These data suggest that AvrRps4 separates RRS1 DOM4 from D56 during activation of the immune complex. The RRS1 fusion protein accumulation is unaltered when coexpressed with AvrRps4 or effector mutants compared with the mCherry control (*SI Appendix*, Fig. S5G), indicating the reduced BiFC signal is not caused by destabilization of RRS1.

We also tested the effect of AvrRps4 on cCFP:D456-R:nVenus BiFC signal. Compared with cCFP:D456-R:nVenus coexpressed with mCherry, coexpression with AvrRps4 but not EEAA significantly reduces the cCFP:D456-R:nVenus BiFC signal in nuclei (*SI Appendix*, Fig. S5 H and I). Coexpression of KRVY also suppresses the BiFC signal of cCFP:D456-R:nVenus, although to a lesser extent compared with AvrRps4 (*SI Appendix*, Fig. S5 H and I). We confirmed that the overall expression level of AvrRps4 is indistinguishable from EEAA or KRVY (*SI Appendix*, Fig. S5J). These observations are consistent with the co-IP data (Fig. 3C), together suggesting that AvrRps4 disrupts DOM4–D56-R association via its interactions with DOM5, thus interfering with the closed conformation of D456-R.

Since the full-length RRS1-R(cCFP-nVenus) is nonresponsive to PopP2, we investigated the effect of PopP2 on D456-R. Neither PopP2 nor C321A interferes with the BiFC signal of cCFP:D456-R:nVenus (Fig. 5E). We also tested the effect of PopP2 on D456-S and observed no significant changes of cCFP:D456-S:nVenus BiFC signal in the presence of PopP2 or C321A (Fig. 5 E

and F). The expression levels of PopP2 and C321A are not different (Fig. 5G).

Overall, we can thus distinguish domain configurations of RRS1 D456 before and after activation. Co-IP results show a negative correlation between DOM4–WRKY association affinity and immune complex activity. BiFC data reveal a decrease in proximity of D456 N and C termini upon activation. We therefore infer a change from closed to open conformation of D456 domains during activation. AvrRps4 shows stronger interference with D456 conformation in co-IP than PopP2, and PopP2 shows no interference in BiFC, supporting the idea that AvrRps4 acts differently to PopP2 to activate the immune complex.

**FRET Analyses Reveal Differences in RRS1 D456 Conformation Preactivation and Postactivation.** To complement the BiFC method and to monitor dynamic changes of D456 upon activation, we established an in vivo FRET system. In FRET, the energy transfer from donor fluorophores (eCFP) to nearby acceptor fluorophores (YFP) occurs through a dynamic and reversible dipole-to-dipole coupling, and can be quantified using acceptor photobleaching (FRET-AB). This provides a powerful tool to detect small changes in proximity. We anticipate the FRET efficiencies of eCFP:D456-R:YFP would reflect a range of open (lower FRET) or closed (higher FRET) states of D456-R (Fig. 6A). To eliminate the variability of cotransformation efficiency, we built constructs carrying eCFP:D456-R:YFP with AvrRps4:mCherry, or with controls 35S:mCherry, EEAA:mCh and KRVY:mCh, on the same T-DNA (Fig. 6B). We observed high FRET efficiencies of eCFP:D456-R:YFP (average, ~31%) with mCh, and AvrRps4 significantly lowers this FRET efficiency (average ~25.4%), indicating reduced proximity between N and C termini of D456 and therefore a more open conformation (Fig. 6C). In contrast to AvrRps4, the presence of EEAA does not significantly reduce the FRET efficiency compared with mCh (Fig. 6C). KRVY decreases the FRET efficiency to a level intermediate between AvrRps4 and EEAA, but not significantly different from either (Fig. 6C). We compiled FRET efficiency of single-cell measurements from different biological replicates, and compared the means to establish statistical significance (Fig. 6C and *SI Appendix*, Table S2).
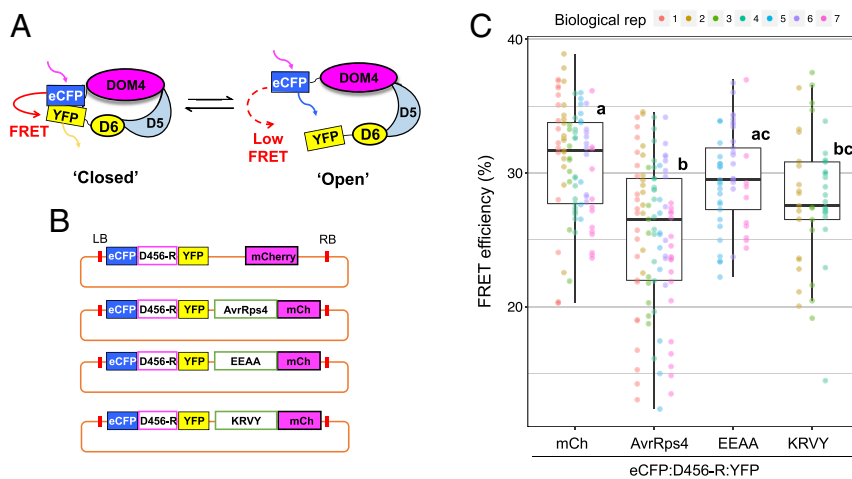


**Fig. 6.** FRET analyses reveal differences in RRS1 D456 conformation preactivation and postactivation. (*A*) Cartoon illustrates how FRET reflects possible conformational differences of eCFP:D456-R:YFP. (*B*) Diagrams illustrate plasmid design for FRET assays. LB and RB indicate T-DNA left and right borders, respectively. For simplicity, details of the promoters and terminators are omitted from the cartoon and are in *SI Appendix*. (*C*) FRET efficiency of eCFP:D456:YFP is significantly reduced in the presence of AvrRps4 and AvrRps4(KRVY), but not AvrRps4(EEAA), compared with mCherry(mCh) control. FRET analyses were performed after transient expression of described constructs (*B*) in *Nb* leaves at 2 dpi. Data points, pooling several biological replicates, each represents a single-cell FRET efficiency (in percentage) quantified by FRET-AB. Linear mixed-effects model (lme) and tests for general linear hypotheses (glht) with Tukey comparisons were used for statistical analysis. Means with the same letter are not significantly different (*P* < 0.001).
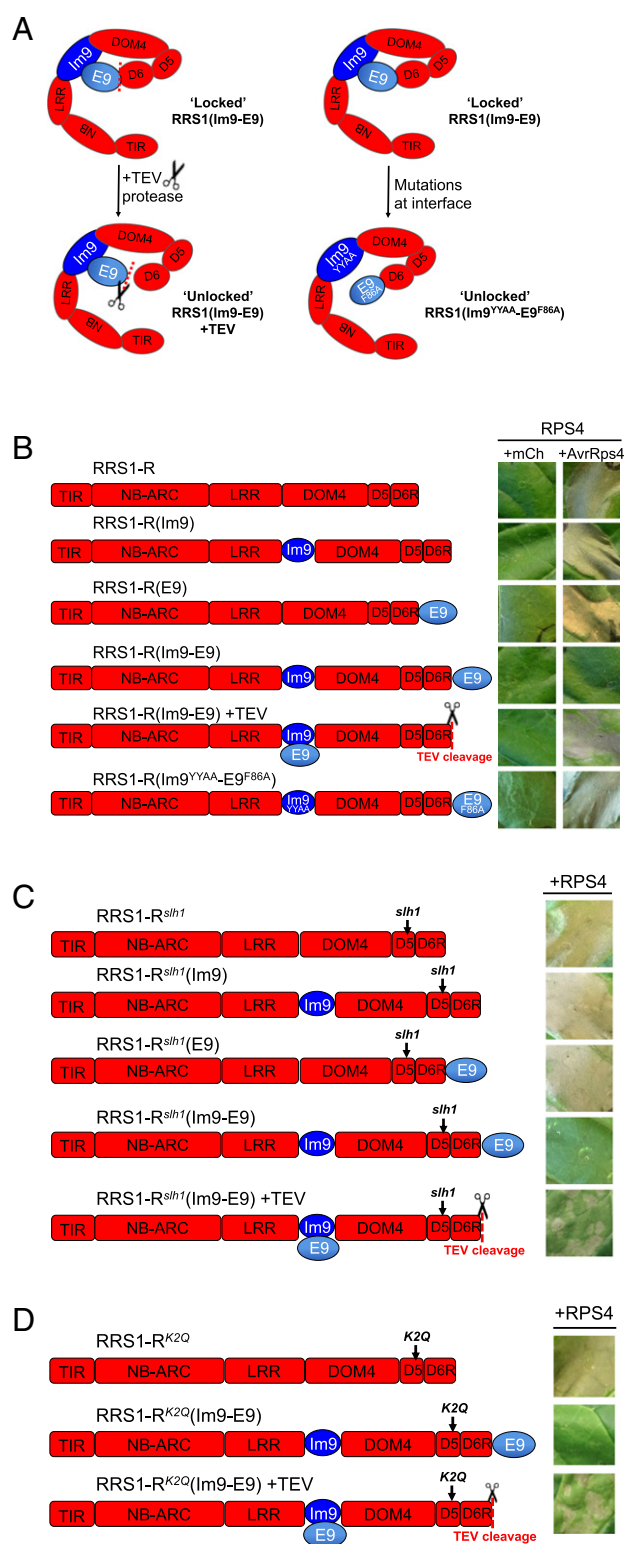
Ma et al.

We also tested whether the autoactive domain swaps D456 (ABA) and D456(ABB) affect the conformation of D456-R. In BiFC assays, both cCFP:D456(ABA):nCer and cCFP:D456 (ABB):nCer produce significantly lower signals than cCFP: D456-R(AAA):nCer (*SI Appendix*, Fig. S6 *A and B*). We confirmed in FRET assays that eCFP:D456(ABA):YFP and eCFP: D456(ABB):YFP show significantly lower FRET efficiencies than eCFP:D456-R(AAA):YFP (*SI Appendix*, Fig. S6C). These data indicate the chimeric domains D456(ABA) and D456 (ABB) show reduced proximity of their N and C termini compared with D456-R(AAA), possibly due to lower affinity between DOM4(A) and D56(BB) or D56(BA). Notably, cCFP: D456(BBB):nCer produces no BiFC signal (*SI Appendix*, Fig. S6 *A and B*), consistent with the lack of DOM4(B) and D56(BB) interactions in co-IP (*SI Appendix*, Fig. S3A), suggesting that D456(BBB) of RRS1B has a different conformation compared with RRS1.

Overall, co-IP, BiFC, and FRET experiments demonstrate that AvrRps4 but not PopP2 can disrupt WRKY association with DOM4 of RRS1. We suggest this disruption makes a key contribution to RRS1-R–RPS4 complex activation by AvrRps4, but that activation via PopP2 acetylation of the WRKY domain is via more subtle conformational changes that require the participation of the longer domain 6 in RRS1-R.

**Engineered RRS1-R with a Reversibly Closed D456-R Shows Reversible Loss of Defense Activation.** To test further whether conformational changes of RRS1 D456-R are essential for defense activation, we engineered a reversible "molecular lock" around RRS1-R D456-R. The "lock" comprises *Escherichia coli* colicin and immunity proteins that interact with high affinity (dissociation constant, $\sim10^{-16}$ M). We used an enzymatically inactive form of the colicin E9 endonuclease (E9), and its cognate inhibitor immunity protein, Im9 (36). Inserting Im9 and E9 within a full-length RRS1-R at the N and C termini of D456-R, forming RRS1-R(Im9-E9), locks D456-R in closed conformation (Fig. 7A). To achieve reversibility, we included a tobacco etch virus (TEV) cleavage site between DOM6 and the N terminus of E9, which allows "unlocking" in the presence of TEV protease (Fig. 7A).

We first confirmed that insertion of Im9 between the LRR domain and D456-R, forming RRS1-R(Im9), or fusion of E9 at the C terminus, forming RRS1-R (E9), does not compromise autoinhibition or AvrRps4 responsiveness of RRS1-R (Fig. 7B). Intriguingly, only when the N and C termini of D456-R are simultaneously tagged with Im9 and E9 [RRS1-R(Im9-E9)], AvrRps4 responsiveness is lost. This was largely restored by coexpressing TEV protease, suggesting that cleavage-dependent relief of the "locked" D456-R allows conformational changes in D456-R that are necessary for AvrRps4-triggered activation (Fig. 7B). As an additional control, we introduced mutations at the E9/Im9 interface, Y54A, Y55A (Im9$^{YYAA}$), and F86A (E9$^{F86A}$), to abrogate their interaction (36). We found that RRS1-R(Im9$^{YYAA}$-E9$^{F86A}$) together with RPS4 responds like RRS1-R to AvrRps4, suggesting that tagging with "nonsticky" E9 and Im9 does not interfere with AvrRps4-triggered conformational changes in RRS1-R (Fig. 7 *A and B*). We confirmed accumulations of these engineered RRS1-R proteins, before and after TEV cleavage (*SI Appendix*, Fig. S7A).

**Fig. 7.** Engineered RRS1-R with a reversibly closed D456-R shows reversible loss of defense activation. (*A*) Schematic overview of RRS1-R engineering. Tagging the N and C termini of D456-R within a full-length RRS1-R with high-affinity proteins Im9 and E9 imposes a closed D456-R conformation. A TEV cleavage site at the N terminus of E9 is designed to allow cleavage and thus relieves this closed conformation upon coexpression of TEV protease. Interface mutants Im9$^{YYAA}$ and E9$^{F86A}$ that abolish Im9–E9 interactions were used to engineer a control open RRS1-R. (*B*) Engineered RRS1-R with a reversibly closed D456-R shows reversible loss of defense activation by AvrRps4. Each tobacco leaf section was coinfiltrated to transiently express RPS4 and an engineered RRS1-R with mCherry (mCh) or AvrRps4. RRS1-R(Im9) carries an Im9 between LRR and DOM4. RRS1-R(E9) contains an E9 fused to the C terminus. RRS1-R(Im9-E9) and RRS1-R(Im9$^{YYAA}$-E9$^{F86A}$) are simultaneously tagged with Im9 and E9 or their mutants, respectively. (*C* and *D*) Engineered RRS1-R$^{slh1}$ or RRS1-R$^{K2Q}$ with a reversibly closed D456-R shows reversible loss of autoactivity. Each leaf section was coinfiltrated to express RPS4 with an engineered RRS1-R$^{slh1}$ or RRS1-R$^{K2Q}$. HRs were assessed at 4 dpi. Photographs are representative of three consistent replicates.

To distinguish whether the loss of AvrRps4 responsiveness by RRS1-R(Im9-E9) results from Im9–E9 interaction within one molecule (intramolecular) or between two molecules (intermolecular), we coinfiltrated RRS1-R(Im9) and RRS1-R(E9) with RPS4 (*SI Appendix*, Fig. S7B). AvrRps4 responses are uncompromised, suggesting that Im9 and E9 interactions between two different RRS1-R molecules do not compromise defense activation (*SI Appendix*, Fig. S7C). This is consistent with our data showing that the closed confirmation of D456-R is maintained via domain interactions within, rather than between, RRS1-R molecules (*SI Appendix*, Fig. S5 *C–E*).

In contrast, PopP2 responsiveness is impaired but not abolished by C-terminal tagging with E9 in RRS1-R(E9) (*SI Appendix*, Fig. S7 *D* and *E*), again indicating an important requirement for DOM6-R in PopP2 but not AvrRps4 responsiveness. Compared with RRS1-R, RRS1-R(Im9) + RPS4 has a weaker response to PopP2, although not as weak as RRS1-R(E9). RRS1-R(Im9-E9) + TEV and RRS1-R(Im9$^{YYAA}$-E9$^{F86A}$) together with RPS4 also lack PopP2 responses (*SI Appendix*, Fig. S7 *D* and *E*). This suggests that PopP2 responsiveness is more sensitive to structural alterations of RRS1-R compared with AvrRps4, consistent with the lack of PopP2 responses by RRS1-R(cCFP-nVenus) (Fig. 5*A*).

We similarly engineered E9 and Im9 into the autoactive alleles RRS1-R$^{slh1}$ and RRS1-R$^{K2Q}$. When either N or C terminus of D456-R of RRS1-R$^{slh1}$ was tagged with E9 or Im9, respectively, its autoimmune phenotype was unaltered (Fig. 7*C*). In contrast, the RPS4-dependent autoactivity was completely lost in RRS1-R$^{slh1}$(Im9-E9) or RRS1-R$^{K2Q}$(Im9-E9) (Fig. 7 *C* and *D*), suggesting that "locked closed" D456 can prevent constitutive defense activation triggered by mutations in the WRKY domain (*slh1*, *K2Q*). Furthermore, "unlocking D456-R" by coexpressing TEV partially restores their autoactivity (Fig. 7 *C* and *D*). Conceivably, the detached E9 after TEV cleavage interacts with the Im9 embedded in RRS1-R, which might reduce complex activation, causing a weaker HR.

Validation of functional relevance of conformational changes is a nontrivial challenge. By engineering RRS1-R with a cleavable molecular lock, we were able to reversibly close D456-R, demonstrating that conformational changes of D456 are essential for AvrRps4-triggered activation. This Im9/E9 reversible protein engineering tool opens avenues for investigating conformational change of immune receptors during activation and is broadly applicable to many other protein complexes.

## Discussion

How paired NLRs convert effector recognition into defense activation is poorly understood. We hypothesize that, upon effector perception, the sensor NLR activates a chain of domain reconfigurations that derepress the executor NLR, eventually allowing its signaling domain to activate defense. In the absence of structural knowledge, obtaining insights into conformational changes of multidomain protein complexes is challenging.

We addressed this challenge in the RPS4–RRS1 system. Using deletions and domain swaps, we found that the sensor WRKY domain negatively regulates the RPS4–RRS1 complex. Biochemical and cell biology data support a model in which AvrRps4 derepresses RRS1 via disrupting DOM4–WRKY association, enabling D456 to activate via the RPS4 CTD. PopP2-triggered activation is less easily explained by such disruptions and likely involves the longer DOM6 of RRS1-R. We propose that PopP2 acetylation of the WRKY domain derepresses DOM6 of RRS1-R, allowing to alter D456–CTD interactions via mechanisms that are different from AvrRps4. These observations show that a crucial contribution to RPS4–RRS1 activation is derepression of RRS1 D456.

To investigate dynamic changes of NLR domains upon effector treatment, we used FRET, which is more sensitive and quantitative in spatial comparisons. We observed a gradient of FRET efficiency with or without AvrRps4. Conceivably, D456 fluctuates between closed and open conformations, and effector engagement promotes accumulation of the active form, eventually activating RPS4. This fits with the equilibrium model described for L6 (10), which could also apply to multipartner NLR complexes, highlighting a threshold for activation determined by gradual conformational changes. The end point for defense activation is likely to be oligomerization of the RPS4 TIR domain, but other components of the complex may also contribute. Importantly, although expression of RPS4 alone can activate HR (37), a much stronger HR is seen upon activation of the RPS4–RRS1-R complex by an effector, and thus immune complex activation is not a simple derepression of an executor but also involves activation of RPS4 by RRS1.

Domain swap analysis suggests that DOM4 of RRS1-R and CTD of RPS4 coevolved to mediate signal transduction between the sensor and executor. Although DOM4(A) coimmunoprecipitates with CTD(B), and DOM4(B) with CTD(A), DOM4 or CTD swaps between A and B pair proteins can result in immune complexes unable to respond to effectors. Intriguingly, homologous sequences of DOM4 and CTD are found in other paired TNLs that are arranged in a head-to-head orientation, such as *CHS3/CSA1*, *CHS1/SOC3*, *At4g12010/At4g12020*, *At4g19530/At4g19520*, *At3g51570/At3g51560*, and *At4g36150/At4g36140* (31, 38, 39), implying a conserved coupling of DOM4-like and CTD-like domains in paired TNLs. We speculate that DOM4 and CTD might enable the sensor to activate the executor in other TNL pairs.

Interestingly, *RRS1*-like genes lacking a WRKY domain are found in *Arabidopsis lyrata* and *Brassica rapa* (26), perhaps resembling an ancestral *Arabidopsis thaliana* (At) *RRS1* before the WRKY integration event. Each are adjacent to an *RPS4*-like gene, but these WRKY-lacking *RRS1*-like genes do not cause autoactivation of defense. Thus, we speculate that the WRKY domain initially fused to an ancestral *AtRRS1* was not required for autoinhibition, and its pivotal role in negatively regulating the immune complex likely evolved gradually. The integrated WRKY domains evolve toward the optimal balance at which they are sensitive enough to activate a signaling response rapidly upon effector detection, while limiting inappropriate activation in the absence of a pathogen. Consistent with this idea, we found that appropriate interactions between WRKY and DOM4 of RRS1 are required for autoinhibition, and an independently evolved RRS1B WRKY domain is incompatible for such interactions when swapped into RRS1, resulting in autoactivity.

IDs play a crucial role in NLR activation. They can act both as the effector sensor and as a central regulator, allowing rapid yet specific activation in response to pathogen perception. Consistent with this, a mutation in an ID of CHS3 also results in autoimmunity, which is dependent on the linked RPS4-like CSA1 (38), suggesting that this ID also negatively regulates this paired TNL. The discovery of NLR-IDs raised the exciting possibility of engineering synthetic resistance genes in which the ID in an NLR is replaced with another ID that is also a pathogen target. However, our data suggest that it will not be easy to engineer new IDs into RRS1-R without creating RPS4-dependent constitutively active alleles. Better understanding of how IDs regulate immune receptors would help to uncouple the regulatory requirements from their effector detection capacities and better inform resistance engineering.

## Materials and Methods

The materials and methods used in this study are described in detail in *SI Appendix, SI Materials and Methods*, including plant materials, cloning details for plasmid construction, and protein engineering. It also includes detailed information regarding tobacco transient assays, immunoblot analysis, co-IP assays, BiFC assays, and FRET assays, and quantification and statistical analysis.

1. Dangl JL, Jones JD (2001) Plant pathogens and integrated defence responses to infection. *Nature* 411:826–833.
2. van der Hoorn RA, Kamoun S (2008) From guard to decoy: A new model for perception of plant pathogen effectors. *Plant Cell* 20:2009–2017.
3. Duxbury Z, et al. (2016) Pathogen perception by NLRs in plants and animals: Parallel worlds. *BioEssays* 38:769–781.
4. Jones JD, Vance RE, Dangl JL (2016) Intracellular innate immune surveillance devices in plants and animals. *Science* 354:aaf6395.
5. Jones JD, Dangl JL (2006) The plant immune system. *Nature* 444:323–329.
6. Takken FL, Albrecht M, Tameling WI (2006) Resistance proteins: Molecular switches of plant defence. *Curr Opin Plant Biol* 9:383–390.
7. Maekawa T, et al. (2011) Coiled-coil domain-dependent homodimerization of intracellular barley immune receptors defines a minimal functional module for triggering cell death. *Cell Host Microbe* 9:187–199.
8. Maekawa T, Kufer TA, Schulze-Lefert P (2011) NLR functions in plant and animal immune systems: So far and yet so close. *Nat Immunol* 12:817–826.
9. Sukarta OCA, Slootweg EJ, Goverse A (2016) Structure-informed insights for NLR functioning in plant immunity. *Semin Cell Dev Biol* 56:134–149.
10. Bernoux M, et al. (2016) Comparative analysis of the flax immune receptors L6 and L7 suggests an equilibrium-based switch activation model. *Plant Cell* 28:146–159.
11. Swiderski MR, Birker D, Jones JD (2009) The TIR domain of TIR-NB-LRR resistance proteins is a signaling domain involved in cell death induction. *Mol Plant Microbe Interact* 22:157–165.
12. Schreiber KJ, Bentham A, Williams SJ, Kobe B, Staskawicz BJ (2016) Multiple domain associations within the *Arabidopsis* immune receptor RPP1 regulate the activation of programmed cell death. *PLoS Pathog* 12:e1005769.
13. Williams SJ, et al. (2014) Structural basis for assembly and function of a heterodimeric plant immune receptor. *Science* 344:299–303.
14. Bernoux M, et al. (2011) Structural and functional analysis of a plant resistance protein TIR domain reveals interfaces for self-association, signaling, and autoregulation. *Cell Host Microbe* 9:200–211.
15. Baggs E, Dagdas G, Krasileva KV (2017) NLR diversity, helpers and integrated domains: Making sense of the NLR IDentity. *Curr Opin Plant Biol* 38:59–67.
16. Zhang X, Dodds PN, Bernoux M (2017) What do we know about NOD-like receptors in plant immunity? *Annu Rev Phytopathol* 55:205–229.
17. Césari S, et al. (2014) The NB-LRR proteins RGA4 and RGA5 interact functionally and physically to confer disease resistance. *EMBO J* 33:1941–1959.
18. Wu CH, et al. (2017) NLR network mediates immunity to diverse plant pathogens. *Proc Natl Acad Sci USA* 114:8113–8118.
19. Sarris PF, Cevik V, Dagdas G, Jones JD, Krasileva KV (2016) Comparative analysis of plant immune receptor architectures uncovers host proteins likely targeted by pathogens. *BMC Biol* 14:8.
20. Kroj T, Chanclud E, Michel-Romiti C, Grand X, Morel JB (2016) Integration of decoy domains derived from protein targets of pathogen effectors into plant immune receptors is widespread. *New Phytol* 210:618–626.
21. Cesari S, Bernoux M, Moncuquet P, Kroj T, Dodds PN (2014) A novel conserved mechanism for plant NLR protein pairs: The "integrated decoy" hypothesis. *Front Plant Sci* 5:606.
22. Huh SU, et al. (2017) Protein-protein interactions in the RPS4/RRS1 immune receptor complex. *PLoS Pathog* 13:e1006376.
23. Wu CH, Belhaj K, Bozkurt TO, Birk MS, Kamoun S (2016) Helper NLR proteins NRC2a/b and NRC3 but not NRC1 are required for Pto-mediated cell death and resistance in *Nicotiana benthamiana*. *New Phytol* 209:1344–1352.
24. Peart JR, Mestre P, Lu R, Malcuit I, Baulcombe DC (2005) NRG1, a CC-NB-LRR protein, together with N, a TIR-NB-LRR protein, mediates resistance against tobacco mosaic virus. *Curr Biol* 15:968–973.
25. Bonardi V, Tang S, Stallmann A, Roberts M, Cherkis K, Dangl JL (2011) Expanded functions for a family of plant intracellular immune receptors beyond specific recognition of pathogen effectors. *Proc Natl Acad Sci USA* 108:16463–16468.
26. Saucet SB, et al. (2015) Two linked pairs of *Arabidopsis* TNL resistance genes independently confer recognition of bacterial effector AvrRps4. *Nat Commun* 6:6338.
27. Bomblies K, Weigel D (2007) Hybrid necrosis: Autoimmunity as a potential gene-flow barrier in plant species. *Nat Rev Genet* 8:382–393.
28. Chae E, et al. (2014) Species-wide genetic incompatibility analysis identifies immune genes as hot spots of deleterious epistasis. *Cell* 159:1341–1351.
29. Gassmann W, Hinsch ME, Staskawicz BJ (1999) The *Arabidopsis* RPS4 bacterial-resistance gene is a member of the TIR-NBS-LRR family of disease-resistance genes. *Plant J* 20:265–277.
30. Deslandes L, et al. (2003) Physical interaction between RRS1-R, a protein conferring resistance to bacterial wilt, and PopP2, a type III effector targeted to the plant nucleus. *Proc Natl Acad Sci USA* 100:8024–8029.
31. Narusaka M, et al. (2009) RRS1 and RPS4 provide a dual resistance-gene system against fungal and bacterial pathogens. *Plant J* 60:218–226.
32. Le Roux C, et al. (2015) A receptor pair with an integrated decoy converts pathogen disabling of transcription factors to immunity. *Cell* 161:1074–1088.
33. Sarris PF, et al. (2015) A plant immune receptor detects pathogen effectors that target WRKY transcription factors. *Cell* 161:1089–1100.
34. Sohn KH, et al. (2014) The nuclear immune receptor RPS4 is required for RRS1SLH1-dependent constitutive defense activation in *Arabidopsis thaliana*. *PLoS Genet* 10:e1004655.
35. Sohn KH, Hughes RK, Piquerez SJ, Jones JD, Banfield MJ (2012) Distinct regions of the *Pseudomonas syringae* coiled-coil effector AvrRps4 are required for activation of immunity. *Proc Natl Acad Sci USA* 109:16371–16376.
36. Kleanthous C, Walker D (2001) Immunity proteins: Enzyme inhibitors that avoid the active site. *Trends Biochem Sci* 26:624–631.
37. Zhang Y, Dorey S, Swiderski M, Jones JD (2004) Expression of RPS4 in tobacco induces an AvrRps4-independent HR that requires EDS1, SGT1 and HSP90. *Plant J* 40:213–224.
38. Xu F, et al. (2015) Autoimmunity conferred by chs3-2D relies on CSA1, its adjacent TNL-encoding neighbour. *Sci Rep* 5:8792.
39. Zhang Y, et al. (2017) Temperature-dependent autoimmunity mediated by *chs1* requires its neighboring *TNL* gene *SOC3*. *New Phytol* 213:1330–1345.